Neuronal connections of direct and indirect pathways for stable value memory in caudal basal ganglia

Hidetoshi Amita,[1] [ID] Hyoung F. Kim,[2,3] [ID] Mitchell K. Smith,[1] Atul Gopal[1] [ID] and Okihide Hikosaka[1] [ID]

[1]Laboratory of Sensorimotor Research, National Eye Institute, National Institutes of Health, Bethesda, Maryland,
[2]Department of Biomedical Engineering, Sungkyunkwan University (SKKU), Suwon, Korea
[3]Center for Neuroscience Imaging Research, Institute for Basic Science (IBS), Suwon, Korea

Abstract

Direct and indirect pathways in the basal ganglia work together for controlling behavior. However, it is still a controversial topic whether these pathways are segregated or merged with each other. To address this issue, we studied the connections of these two pathways in the caudal parts of the basal ganglia of rhesus monkeys using anatomical tracers. Our previous studies showed that the caudal basal ganglia control saccades by conveying long-term values (stable values) of many visual objects toward the superior colliculus. In experiment 1, we injected a tracer in the caudate tail (CDt), and found local dense plexuses of axon terminals in the caudal-dorsal-lateral part of substantia nigra pars reticulata (cdlSNr) and the caudal-ventral part of globus pallidus externus (cvGPe). These anterograde projections may correspond to the direct and indirect pathways, respectively. To verify this in experiment 2, we injected different tracers into cdlSNr and cvGPe, and found many retrogradely labeled neurons in CDt and, in addition, the caudal-ventral part of the putamen (cvPut). These cdlSNr-projecting and cvGPe-projecting neurons were found intermingled in both CDt and cvPut (which we call "striatum tail"). A small but significant proportion of neurons (<15%) were double-labeled, indicating that they projected to both cdlSNr and cvGPe. These anatomical results suggest that stable value signals (good vs. bad) are sent from the striatum tail to cdlSNr and cvGPe in a biased (but not exclusive) manner. These connections may play an important role in biasing saccades toward higher valued objects and away from lower valued objects.

Introduction

The basal ganglia have two main parallel pathways, that is, direct and indirect pathway. The input structures of the basal ganglia, which include the caudate nucleus (CD) and the putamen (Put), have direct projections to the output structures, including the substantia nigra pars reticulata (SNr) and the globus pallidus internus (GPi). In addition, these input structures also have indirect projections to the output structures through the globus pallidus externus (GPe) and the subthalamic nucleus (STN).

These two pathways are likely to work as an antagonistic pair because they have different connection patterns (DeLong, 1990; Hikosaka, Takikawa, & Kawagoe, 2000; Mink, 1996). Through the direct pathway, excitation of the input structures (CD and Put) would lead to inhibition of the output structures (SNr and GPi). Through the indirect pathway, excitation of the input structures would lead to disinhibition (i.e., excitation) of the output structures. Recent studies indicate that these two pathways have opposing and distinct roles in controlling

behavior (Ferguson et al., 2011; Hikida, Kimura, Wada, Funabiki, & Nakanishi, 2010; Kravitz, Tye, & Kreitzer, 2012; Kravitz et al., 2010). Activation of direct-pathway striatal neurons facilitates locomotion and reinforcement learning, in contrast to the activation of indirect-pathway neurons which elicits freezing and aversive learning. On the other hand, other recent studies indicate that these two pathways coordinate together during body movements (Cui et al., 2013; Isomura et al., 2013; Jin, Tecuapetla, & Costa, 2014).

The studies introduced above have focused on circuits and functions of the rostral parts of the basal ganglia. However, the direct and indirect pathways in "caudal basal ganglia" are still unclear. The caudal basal ganglia, which includes the caudate tail (CDt), the caudal-dorsal-lateral part of SNr (cdlSNr) and the caudal-ventral part of GPe (cvGPe), are specifically involved in long-term value coding of visual objects (i.e., stable value memory) for saccadic eye movements based on historical life experiences (Kim, Amita, & Hikosaka, 2017; Yamamoto, Kim, & Hikosaka, 2013; Yasuda, Yamamoto, & Hikosaka, 2012). Most neurons in CDt, cdlSNr and cvGPe discriminate visual objects based on their historical value: objects previously and consistently associated with a large reward (good objects) and objects associated with a small reward (bad objects) (Kim et al., 2017).

The next step in elucidating the mechanisms of the stable value memory is to investigate how these structures are interconnected in the caudal basal ganglia. Our previous studies suggest that good

objects facilitate saccades through the direct pathway, while bad objects suppress saccades through the indirect pathway (Hikosaka, Ghazizadeh, Griggs, & Amita, 2017; Kim et al., 2017). The functional difference between direct and indirect pathways might arise due to the anatomical segregation of these pathways. In this paper, we investigated how the caudal basal ganglia structures are organized into the direct and indirect pathways. We also tested whether the same or different neurons in the input structures project to each target through the direct and indirect pathways.

Here, we conducted two experiments to address these questions. First, we identified the efferent structures, cdlSNr and cvGPe innervated by CDt through the direct and indirect pathways by investigating anterogradely labeled axon terminals with tracer injected in CDt. Second, we identified the precise location of neurons projecting to cdlSNr and cvGPe, and potential double-labeling of CDt neurons innervating both cdlSNr and cvGPe by investigating retrogradely labeled neurons with tracers. This study identified the neuronal connections of the direct and indirect pathways which are involved in the stable value memory.

Materials and Methods

Materials and subjects

In experiment 1, histology sections of an adult male rhesus monkey (*Macaca mulatta*, monkey SM used in the previous studies (Kim & Hikosaka, 2013; Kim, Ghazizadeh, & Hikosaka, 2014; Griggs et al., 2017)) was used for immunohistochemistry experiment. In experiment 2, two adult male rhesus monkeys (*Macaca mulatta*, monkeys AX and CR) were used for behavioral tasks, neuronal recording, tracer injection and anatomical analysis. Monkey AX was used in previous studies for neuronal recording and anatomical analysis (Kim et al., 2017; Yasuda & Hikosaka, 2015). All animal care and experimental procedures were approved by the National Eye Institute Animal Care and Use Committee and complied with the Public Health Service Policy on the humane care and use of laboratory animals.

Surgeries for implanting a plastic head holder, plastic recording chambers and scleral search coils were performed in veterinary operating facility using aseptic procedures. Five minutes after the animal was given atropine (0.04 mg/kg, i.m.), anesthesia was induced with ketamine hydrochloride (10 mg/kg, i.m.) along with diazepam (0.2 mg/kg, i.m.) and maintained using isoflurane gas (1.5%–3% to effect). Vital signs were monitored throughout the surgeries. The animal's head was placed in a stereotaxic frame. The head holder and chambers were positioned with manipulators onto the skull and affixed with dental cement. The search coil was placed under the conjunctiva. To prevent post-operative swelling after the search coil implantation, antibiotic ointment was placed on the conjunctiva. The post-operative animals were carefully observed. The wound margin was cleaned with betadine-saline solution (2%) and healed by application of antibiotic ointment. After 6 weeks of recovery, behavioral training began. A craniotomy inside the recording chamber was performed and the dura mater was exposed in the chamber to enable neuronal recording. The chamber was cleaned with saline solution and covered with a chamber cap. Chambers were cleaned by flushing with only saline solution at least three times a week until recovery, and then routinely cleaned by flushing with hydrogen peroxide or a mixture of betadine and saline solution at least three times a week.

Anatomical tracer injection

We injected different tracers in different parts in the CDt-circuit (Table 1) in order to achieve several goals, as described below.

TABLE 1. Bi-directional tracers and injection sites

Monkey	CDt	cdlSNr	cvGPe	Hemisphere
SM	CTB555	(–)	(–)	Right
AX	(–)	CTB488	(–)	Left
AX	(–)	FB	CTB555	Right
CR	(–)	CTB488	CTB555	Right

In experiment 1, we injected a tracer in CDt in monkey SM to find brain areas that are innervated by CDt (Figure 1; Table 1). We used a bi-directional tracer, cholera toxin subunit B conjugated with Alexa Fluor 555 (CTB555; C22843; Life technologies). We determined the injection site by recording single neuronal activity. We used a custom-made injectrode consisting of an epoxy-coated tungsten microelectrode (200 μm thick; FHC, Bowdoin, ME, USA) for neuronal recording and a silica tube (outer/inner diameter: 155/75 μm; Polymicro Technologies, Phoenix, AZ, USA) for tracer injection. The tracer injection was made after we found several neurons that responded to visual objects selectively and encoded stable values of the objects. We injected 0.3 μl CTB555 (1% in 0.01 M, pH 7.4 phosphate buffer) at a speed of 0.01 μl/min using a 10 μl Hamilton syringe attached to a 30-gauge stainless steel needle held in a manual infusion pump (Stoelting, Wood Dale, IL, USA). The injection site was 13 and 14 mm posterior to the anterior commissure (P13-14).

In experiment 2, we injected tracers in two brain areas (cvGPe and cdlSNr) (Table 1) which were shown to receive inputs from CDt in experiment 1. The main goal was to find which brain areas (in addition to CDt) and which neurons project to cvGPe or cdlSNr. Here, we also determined the injection site by recording single neuronal activity using the injectrode. As bi-directional tracers, we used Fast Blue (FB; 17740; Polysciences, Warrington, PA, USA), cholera toxin subunit B conjugated with Alexa Fluor 488 (CTB488; C22841; Life technologies) and 555 (CTB555; C22843; Life technologies). In monkey AX (Table 1), we injected 0.4 μl FB (3% in distilled water) in the right cdlSNr (P12), 0.4 μl CTB488 (1% in 0.01 M, pH 7.4 phosphate buffer) in the left cdlSNr (P14) and 0.3 μl CTB555 (1% in 0.01 M, pH 7.4 phosphate buffer) in the right cvGPe (P8) at a speed of 0.01 μl/min using a 10 μl Hamilton syringe held in the manual infusion pump. In monkey CR (Table 1), we injected 0.3 μl CTB488 (1% in 0.01 M, pH 7.4 phosphate buffer) and 0.3 μl CTB555 (1% in 0.01 M, pH 7.4 phosphate buffer) in the same manner except for using a motorized infusion pump (Harvard Apparatus, Holliston, MA, USA). Each of CTB488 and CTB555 were injected in the right cdlSNr (P13-14) and right cvGPe (P9), respectively.

Histology

Two weeks after the tracer injection, monkeys SM, AX and CR were deeply anesthetized with an overdose of sodium pentobarbital (390 mg/ml) and perfused transcardially with saline followed by 4% paraformaldehyde. The head was fixed to the stereotaxic frame, and the brain was cut into blocks in the coronal plane including midbrain region. The block was post-fixed overnight at 4°C, and then cryoprotected for one week in increasing gradients of glycerol solution (5%, 10% to 20% glycerol in PBS) before being frozen. Frozen block was cut every 50 μm using a microtome. Every 250 μm interval slices were used for cell counting, and the adjacent two slices were used for Nissl staining and taking photomicrographs. The slices were reconstructed according to the locations of the tracer
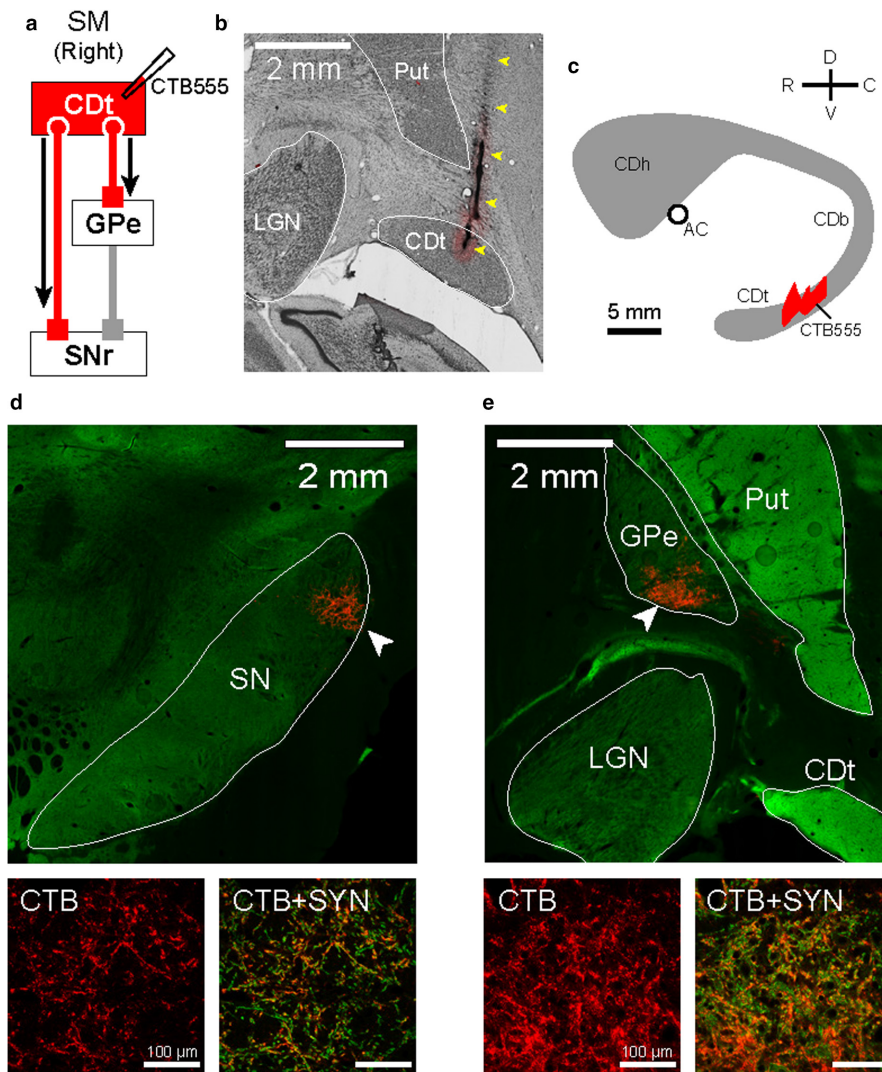
FIG. 1. CDt projected to the caudal parts of SNr and GPe. (a) Scheme of injection site in CDt of monkey SM. CTB555 was injected in CDt to identify its projection regions in the direct and indirect pathways. (b) CTB555 injection site in CDt. Injectrode track is indicated by yellow arrowheads. (c) Schematic injection locations at sagittal plane. CTB555 was injected in the middle region of CDt (see more details in the previous paper Kim et al., 2014). (d) CDt projection site in SNr which is shown by CTB signals (red). This was, localized in the caudal-dorsal-lateral part of SNr (cdlSNr; white arrowhead in top panel). CTB signals in cdlSNr (red in left-bottom panel) were co-localized with synaptophysin (SYN), an axon terminal marker (orange in right-bottom panel). (e) CDt projection site in cvGPe. Axon terminals from CDt were localized in the caudal-ventral part of GPe (cvGPe; white arrowhead in top panel). CTB signals in cvGPe (red in left-bottom panel) were also co-localized with SYN (orange in right-bottom panel).

injection sites, the brain structures and the atlas of the rhesus monkey brain.

Immunofluorescence

We confirmed the axon terminals from CDt (in experiment 1) and cvGPe (in experiment 2) with immunofluorescent double-labeling method. For primary antibodies, we used rabbit anti-CTB (GWB-7B96E4; GenWay Biotech., San Diego, CA, USA) and mouse anti-synaptophysin antibodies (SAB4200544; MilliporeSigma, Burlington, MA, USA). As secondary antibodies, we used goat anti-rabbit IgG antibody conjugated with Alexa Fluor 555 (A-21428; Thermo-Fisher) and goat anti-mouse IgG1 antibody conjugated with Alexa Fluor 488 (A-21121; ThermoFisher).

The sections were preincubated for 30 min in 0.3% hydrogen peroxide in 0.1 M PBS (pH 7.4) to block endogenous peroxidase, followed by three rinses with 0.1 M PBS. Sections were incubated

for 1 hr in blocking solution containing 5% normal goat serum in 0.1 M PBS. The sections were incubated for 18 hr at room temperature in blocking solution containing 2.5% normal goat serum and 0.1% TX-100 with rabbit anti-CTB (1:500) and mouse anti-synaptophysin (1:500) antibody. After three rinses with PBS, the sections were incubated for 2 hr at room temperature with goat anti-rabbit IgG antibody conjugated with Alexa Fluor 555 (1:200) and goat anti-mouse IgG1 antibody conjugated with Alexa Fluor 488 (1:200).

In experiment 2, we enhanced the tracer signals with immunofluorescent double-labeling method. For primary antibodies, we used rabbit anti-Alexa Fluor 488 (A-11094; ThermoFisher) and mouse anti-CTB antibodies (ab62429; abcam, Cambridge, MA, USA). For secondary antibodies, we used goat anti-rabbit IgG antibody conjugated with Alexa Fluor 488 (A-11034; ThermoFisher) and goat anti-mouse IgG1 antibody conjugated with Alexa Fluor 633 (A-21226; ThermoFisher).

The sections were preincubated for 30 min in 0.3% hydrogen peroxide in 0.1 M PBS (pH 7.4) to block endogenous peroxidase, followed by three rinses through 0.1 M PBS, and then 1 hr in blocking solution containing 5% normal goat serum in 0.1 M PBS. The sections were incubated for 18 hr at room temperature in blocking solution containing 2.5% normal goat serum and 0.1% TX-100 with rabbit anti-488 (1:500) and mouse anti-CTB (1:3000) antibody. After three rinses with PBS, the sections were incubated for 2 hr at room temperature with goat anti-rabbit IgG antibody conjugated with Alexa Fluor 488 (1:200) and goat anti-mouse IgG1 antibody conjugated with Alexa Fluor 633 (1:200). We identified the labeled neurons and captured the fluorescence images using a fluorescence microscope (Keyence) and a confocal laser scanning microscope (Zeiss). We adjusted the contrast and brightness of each color channel using software Zen (Zeiss) and Photoshop (Adobe) to enhance the ability to differentiate fluorescently labeled neurons.

Immunohistochemistry

In experiment 2, we examined whether retrogradely labeled cells with CTB488 or CTB555 were localized in patches (striosomes) by potassium channel interacting protein 1 (KChIP1) immunostaining. The sections were preincubated for 10 min in 1% hydrogen peroxide in 0.1 M PBS (pH 7.2) to block endogenous peroxide, followed by three rinses through 0.1 M PBS, and then 1 hr in blocking solution containing 3% normal goat serum and 0.25% TX-100 in 0.1 M PBS. The sections were incubated for 48 hr at 4°C in blocking solution with mouse monoclonal anti-KChIP1 antibody (75-003; NeuroMab, Davis, CA, USA) (1:400). The sections were rinsed three times with PBS, then incubated for 2 hr with biotinylated secondary antibody (PK-6200; Vector Labs, Burlingame, CA, USA) (1:200), washed three times with PBS, and transferred to PBS with peroxidase conjugate from the Vectastain ABC kit (PK-6200; Vector Labs) (1:100). After rinsing three times with PBS, the sections were immersed in a solution containing 0.02% 3,3′-diaminobenzidine tetrahydrochloride hydrate (D5637; Sigma-Aldrich) and 0.003% hydrogen peroxide. After staining, the sections were mounted on glass slides, dehydrated in ethanol, cleared in xylene and coverslipped. We compared sections stained for KChIP1 with adjacent sections labeled with CTB488 or CTB555.

Cell counting

Retrogradely labeled cells were counted manually using a custom software developed in MATLAB (Mathworks). The images from confocal microscope were inspected systematically, and single-labeled (CTB555, CTB488 or FB) or double-labeled neurons were identified. In monkey AX, seven sections (P4, P6, P8, P10, P12, P14 and P16) were analyzed in which 9197 cells (labeled with CTB555) and 4548 cells (with FB) were counted. In monkey CR, six sections (P4, P6, P8, P10, P12 and P14) were analyzed in which 825 cells (with CTB488) and 198 cells (with CTB555) were counted. The overall counts as well as the precise positions of the identified cells were stored for further analysis and reconstruction of the slices.

Results

Caudate tail (CDt) directly projects to cdlSNr and cvGPe

We previously reported that neurons in CDt encoded the stable value of visual objects (Kim & Hikosaka, 2013; Yamamoto et al.,

2013). The goal of experiment 1 was to identify the structures where CDt sends the stable value information. We hence injected a fluorescent tracer CTB555 into CDt in monkey SM (Figure 1a–c), because CTB is a bi-directional tracer which can be taken up by cell bodies as well as axons and transported anterogradely to axon terminals (Chen & AstonJones, 1998). CTB signals were localized as plexuses in cdlSNr and cvGPe (Figure 1d and e, top) which were previously reported (Kim et al., 2017). In addition, we double-labeled the axon plexuses with antibodies against CTB and an axon terminal marker, synaptophysin (SYN) to identify the plexuses as axon terminals. The CTB signals were co-localized with SYN signals (orange signals in Figure 1d and e, bottom). We confirmed that these CTB-labeled plexuses were indeed not passing fibers but axon terminals from CDt. Hence, CDt had direct projections to cdlSNr and cvGPe.

Tracer injections in cdlSNr and cvGPe

The results of experiment 1 suggest that CDt neurons project to cdlSNr through the direct pathway and to cvGPe through the indirect pathway. This result raised two questions. First, are the neurons in CDt projecting to cdlSNr and cvGPe spatially segregated? Second, do the same or different neurons project to cdlSNr and cvGPe?

To address these questions (experiment 2), we first injected different combination of three colored fluorescent tracers (FB, CTB488 and CTB555) in cdlSNr and cvGPe in monkeys AX and CR (Table 1). These tracers are bi-directional (Chen & AstonJones, 1998), but we used them mostly for retrograde labeling in experiment 2. Figure 2a and b show two injection sites in monkey AX.

Since both cdlSNr and cvGPe are small but encode the stable value memory, we identified these structures by single-unit recording with behavioral tasks as previous studies (Kim et al., 2017; Yasuda et al., 2012). Long before the tracer injection, monkeys learned the value of many visual objects, each of which was associated with a large or small reward consistently for more than 5 days (Object-reward associative task, Figure 2c). Then, we identified cdlSNr and cvGPe by recording neuronal activity using passive viewing task (Figure 2d). A majority of neurons in both cdlSNr and cvGPe encoded the stable values of learned objects (Figure 2e and f). Neurons were also functionally identified prior to the tracer injection using the injectrode.

Direct pathway: CDt and cvPut project to cdlSNr

After injecting CTB488 in cdlSNr (Figure 3a), retrogradely labeled cell bodies were found in CDt (Figure 3b), as expected from the anterograde tracer study in experiment 1 (Figure 1d-e). In addition, we found retrogradely labeled neurons in the caudal-ventral part of the putamen (cvPut) (Figure 3b, right). Coronal brain sections in the rostral-caudal axis were examined to identify the retrogradely labeled neurons (Figure 3c-h). We found that cdlSNr-projecting neurons were densely localized through the whole of CDt and cvPut. We further found the labeled neurons less densely localized in the ventral part of caudate body (CDb; Figure 3c-h), the caudal-ventral part of STN (Figure 3e-f), the caudal-ventral part of GPe (Figure 3e-f), the central nucleus of amygdala (CeA; Figure 3c-d), the sublenticular extended amygdala (SLEA; Figure 3c), the bed nucleus of the stria terminalis (BNST; Figure 3c-d) and the ventromedial nucleus of the hypothalamus (VMH; Figure 3c). In the anterior and dorsal parts of CD and Put, a few retrogradely labeled neurons were found. This selective localization of cdlSNr-projecting neurons in CDt and cvPut was reproduced in opposite hemisphere of the same monkey (monkey AX), and in another monkey (monkey
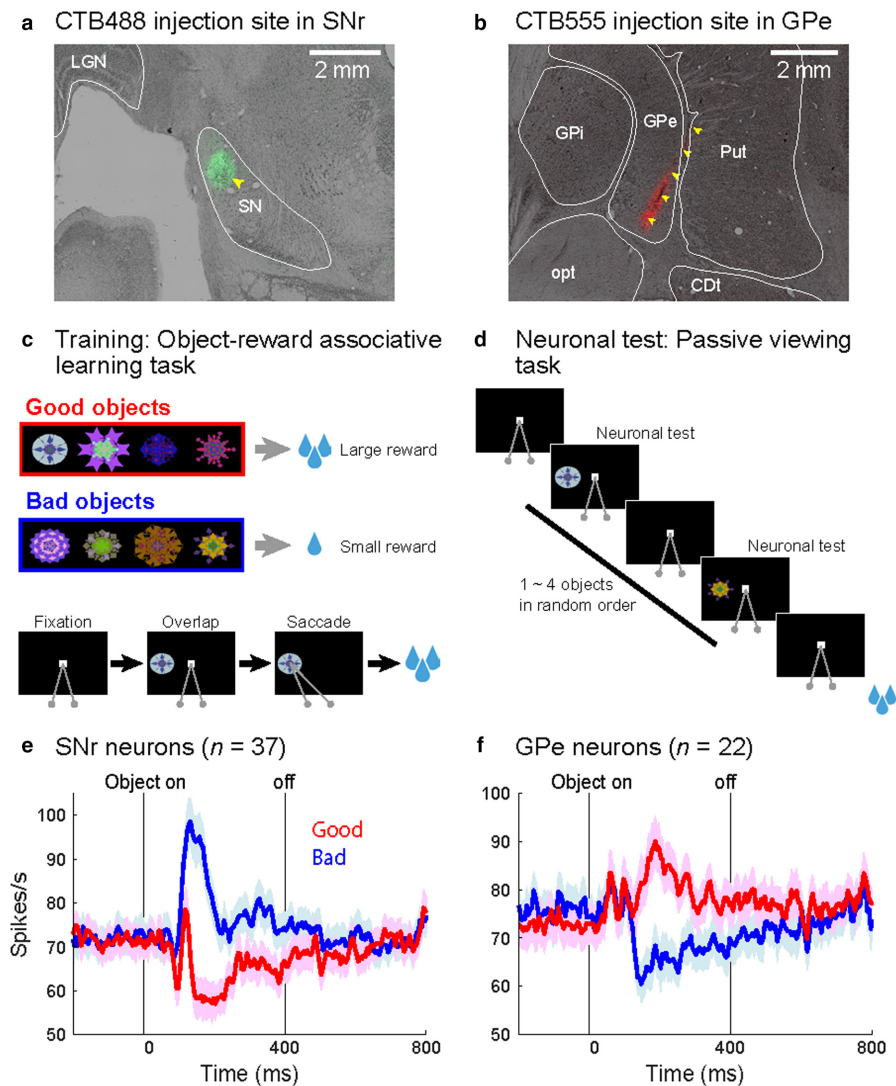
FIG. 2. Task procedures for neuronal test and injection sites showing stable value activities in monkey AX. (a) Injection site in cdlSNr. CTB488 was injected in left cdlSNr (light green area indicated by a yellow arrowhead). (b) Injection site in cvGPe. CTB555 was injected in right GPe (injectrode track indicated by yellow arrowheads). (c) Object-reward associative learning task. An example set of fractal objects that were associated with stable values. Monkeys learned these objects associated with large reward (good objects) or small reward (bad objects) by saccadic eye movements. (d) Passive viewing task. While the monkeys fixated at a central white dot, one to six fractal objects were sequentially presented. Neuronal activity was tested by response to the previously learned good and bad objects in this task. (e) Stable value-coding activity in cdlSNr injection site. In cdlSNr, 37 neurons showed inhibition by good object presentation (red line) and excitation by bad object presentation (blue line). (f) In cvGPe, 22 neurons showed excitation by good objects (red line) and inhibition by bad objects (blue line). Each line indicates the average of firing rate. Each shading area indicates 95% confidence intervals of firing rate. Activities were aligned by the object presentation onset.

CR; Figure 7). In addition, we did not find a clear difference in the distribution of retrogradely labeled neurons between two different tracers, FB and CTB488. These results indicate that the input neurons of the direct pathway in the caudal basal ganglia are fairly localized in caudal-ventral parts of the striatum (i.e., CDt and cvPut).

Indirect pathway: CDt and cvPut project to cvGPe

To identify the area projecting to cvGPe, we examined retrogradely labeled neurons after CTB555 tracer injection in cvGPe (Figure 4a). We found retrogradely labeled neurons in structures of the basal ganglia (Figure 4b). Like cdlSNr-projecting neurons, neurons were densely labeled in CDt and cvPut (Figure 4b, right). Coronal brain sections in the rostral-caudal axis were examined (Figure 5c-h): We

found that cvGPe-projecting neurons were densely localized through the whole of CDt and cvPut (Figure 5c-h). In addition, we found the retrogradely labeled neurons in CeA (Figure 5c-d), SLEA (Figure 5c), VMH (Figure 5c) and centromedian-parafascicular nuclei (CM/Pf) (Figure 5g). The labeling in CM/Pf might be caused by the tracer spread to part of Put (Figure 2b), or by the direct projection of CM/Pf to GPe (Kincaid, Penney, Young, & Newman, 1991; Parent & Parent, 2005; Royce & Mourey, 1985; Sadikot, Parent, Smith, & Bolam, 1992).

To identify the area receiving inputs from cvGPe, we also examined anterogradely labeled plexuses with CTB555 (Figure 5a). We found massive plexuses in cdlSNr anterogradely labeled with CTB555 (Figure 5b). To confirm these plexuses were axon terminals, we double-labeled the plexuses with antibodies against CTB and synaptophysin. These CTB signals were co-localized with
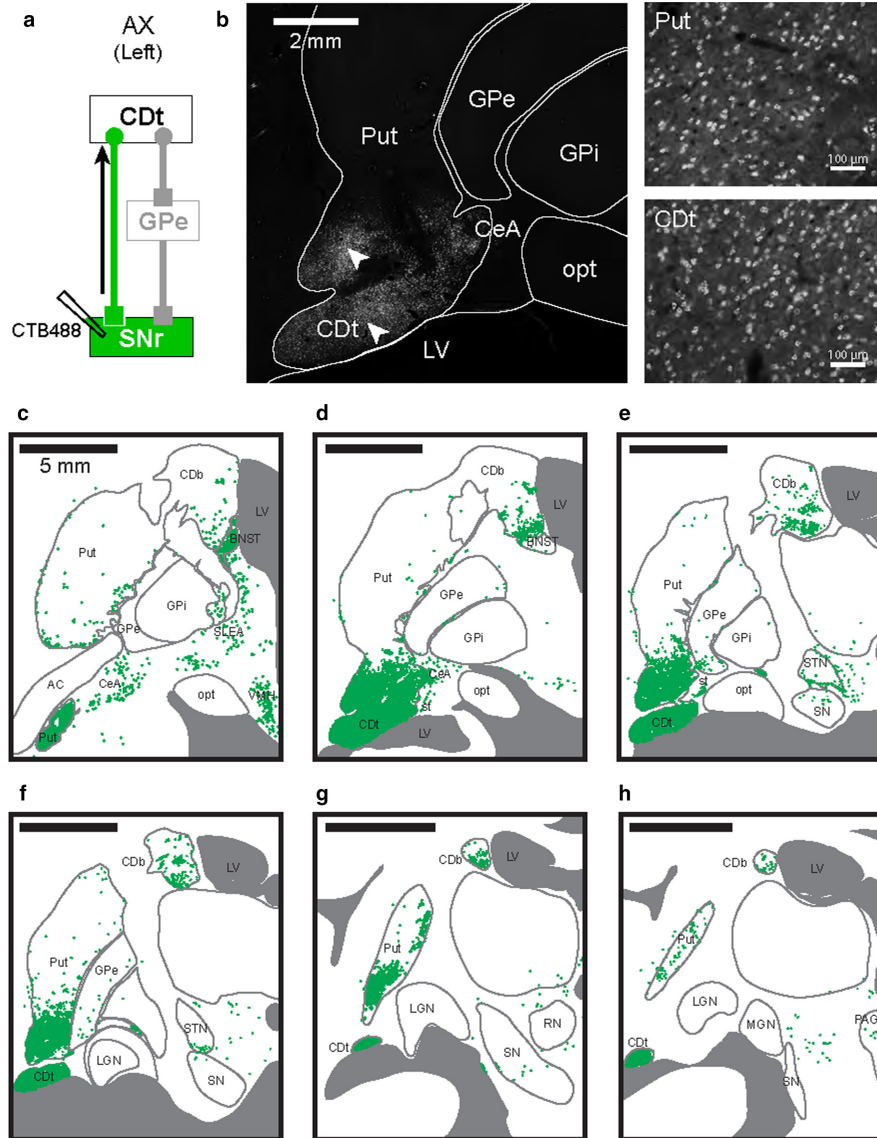
FIG. 3. cdlSNr-projecting neurons in CDt and cvPut. (a) Scheme of injection site in cdlSNr of monkey AX. CTB488 was injected in cdlSNr, and retrogradely labeled neurons in CDt were identified in the direct pathway. (b, left) cdlSNr-projecting neurons in the striatum. Retrogradely labeled neurons (white dots) were densely distributed in Put and CDt. (b, right) Enlarged images of labeled cell bodies in Put and CDt. Enlarged areas where the neurons in cvPut and CDt were retrogradely labeled were CDt indicated by white arrowheads in (b), left. (c-h) Six coronal brain slices (P4, P6, P8, P10, P12 and P14) in the rostral-caudal axis showed neurons retrogradely labeled with CTB488 (green dots). Densely labeled neurons were found through whole parts of CDt and cvPut. Sparsely labeled neurons were found in STN, BNST, VMH, SLEA and CeA. Series of six slices from rostral to caudal at 2 mm intervals.

synaptophysin signals in the cdlSNr (orange signals indicated by white arrowheads in Figure 5c, bottom), confirming that these CTB-labeled plexuses were indeed axon terminals. This shows that cvGPe has direct projections to cdlSNr. These results suggested that the same output structure (i.e., cdlSNr) received inputs through the direct and indirect pathways in the caudal basal ganglia.

Inputs from striatal patches (striosomes)

We so far have indicated that striatal neurons projecting to cdlSNr and cvGPe were localized in its tail part (CDt and cvPut). In detail, however, we found retrogradely labeled cells in patchy areas in the more dorsal and rostral parts of the striatum (Figures 3 and 4). This raised the possibility that these patchy areas correspond to striatal patches (Gerfen, 1984) (also known as striosomes, (Graybiel &

Ragsdale, 1978). To identify the patches (striosomes), we used KChIP1 as a patch (striosome) marker (Mikula, Parrish, Trimmer, & Jones, 2009).

We then compared a section in CDb that included retrogradely labeled cells with CTB488 (Figure 6b, left) with the adjacent section stained by KChIP1 immunostaining (Figure 6b, center). Indeed, most labeled cells were localized in patches (Figure 6b, right), especially those located in the ventral-medial part of CDb. We also found that most retrogradely labeled cells from cvGPe were localized in patches (Figure 6d), especially those located in the middle part of Put. These results suggest that both cdlSNr and cvGPe do receive inputs from CDb and Put, but selectively from patches. This pattern is completely different from the overall inputs from CDt/cvPut (Figures 3 and 4), whose patches (striosomes) were much smaller and sparser than CDb and the middle part of Put (Figure 6d, center).
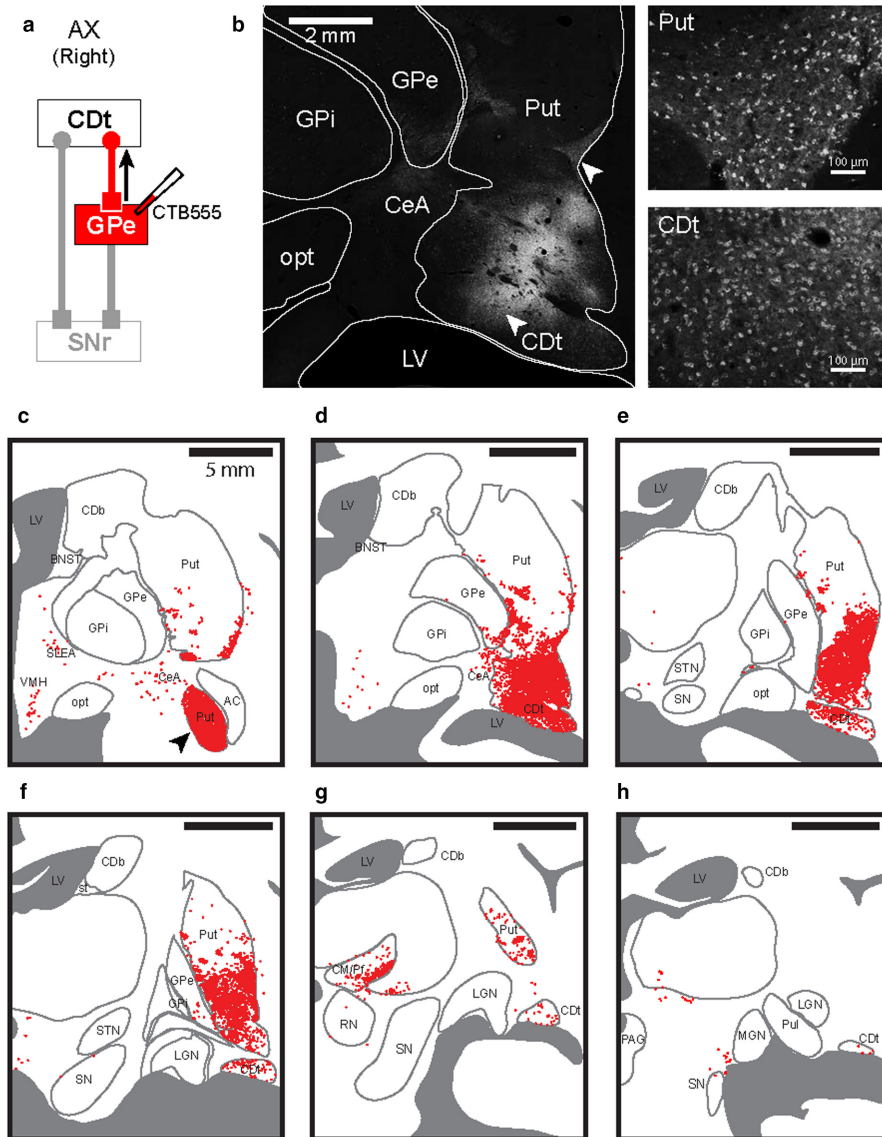
FIG. 4. cvGPe-projecting neurons in CDt and cvPut. (a) Scheme of injection site in cvGPe of monkey AX. CTB555 injected in cvGPe was retrogradely transported along the axons in the indirect pathway. (b, left) cvGPe-projecting neurons in the striatum. Retrogradely labeled neurons (white dots) were densely distributed in Put and CDt. (b, right) Enlarged images of labeled cell bodies in Put and CDt. Enlarged areas where the neurons in cvPut and CDt were retrogradely labeled were indicated by white arrowheads in (b), left. (c-h) Six coronal brain slices (P4, P6, P8, P10, P12 and P14) in the rostral-caudal axis showed densely labeled neurons through whole parts of CDt and cvPut. Sparsely labeled neurons were found in VMH, SLEA and CeA. Series of six sections from rostral to caudal at 2 mm intervals. Black arrowhead in (c) indicates the most rostral part of cvPut, which is also shown in (a).

Target-specific injection of tracers in the second monkey

Results from monkey AX showed that CDt and cvPut were principal structures projecting to cdlSNr and cvGPe. However, the tracer injections were not localized, and part of the tracers had spread to the adjacent areas. To reconfirm the results of monkey AX and identify more specific circuits encoding the stable value memory, we injected tiny amounts of different tracers in both cdlSNr and cvGPe in monkey CR (CTB488 for right cdlSNr and CTB555 for right cvGPe). Anatomical data showed that the injection sites were exclusively localized in cdlSNr and cvGPe (Figure 7a and b). We recorded neuronal activities from these injection sites with the injectrode before each injection. Single neuronal activity at the injection site in cdlSNr was inhibited by good objects and excited by bad objects in the passive viewing task (Figure 7c). In contrast, single neuronal activity at the injection site in cvGPe was inhibited by bad objects (Figure 7d). These data confirmed that the different tracers were selectively injected in stable value-coding regions, cdlSNr and cvGPe of the same monkey.

CTB488 (green) and CTB555 (red) were injected in cdlSNr and cvGPe of the same hemisphere (Figure 8a). Both cdlSNr-projecting neurons (green in Figure 8) and cvGPe-projecting neurons (red in Figure 8) were localized in CDt and cvPut through the coronal brain sections in the rostral-caudal axis (Figure 8b-g), though the number of labeled neurons were much smaller than monkey AX. We further found the cdlSNr-projecting neurons sparsely localized in the CDb (green in Figure 8c-g). These retrograde tracer results with two monkeys suggest two input structures, CDt and cvPut massively project to cdlSNr and cvGPe, which encode the stable value memory, thorough the direct and indirect pathways, and these direct- and indirect-pathway neurons are spatially intermingled in CDt and cvPut.
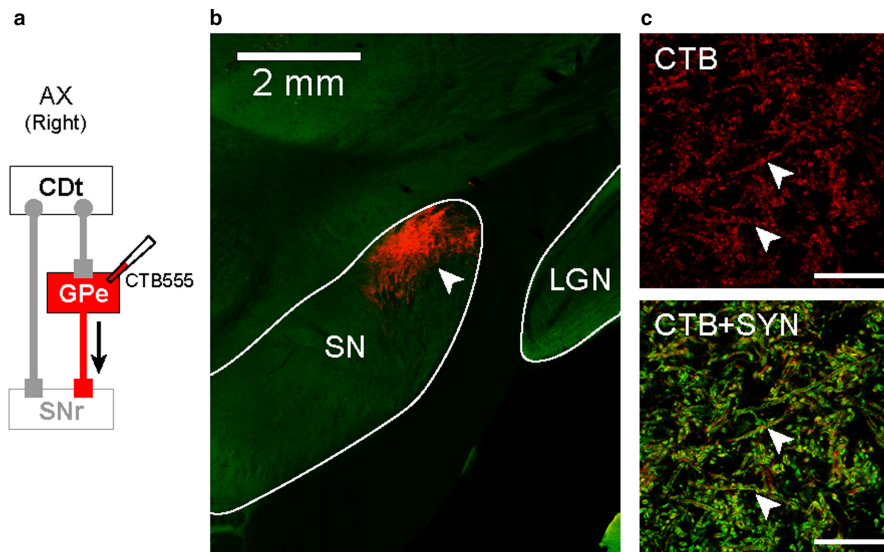
FIG. 5. cvGPe projected to cdlSNr. (a) Scheme of injection site in cvGPe of monkey AX. CTB555 injected in cvGPe was anterogradely transported along the axons. (b) cvGPe projection site in SNr. Anterogradely labeled plexus was localized in the caudal-dorsal-lateral part of SNr (cdlSNr; white arrowhead). (c) SYN-labeled axon terminal of cvGPe in cdlSNr. The anterogradely labeled plexus in cdlSNr (red in top panel) was co-localized with fluorescent signal of SYN (orange signals indicated by white arrowheads in bottom panel).
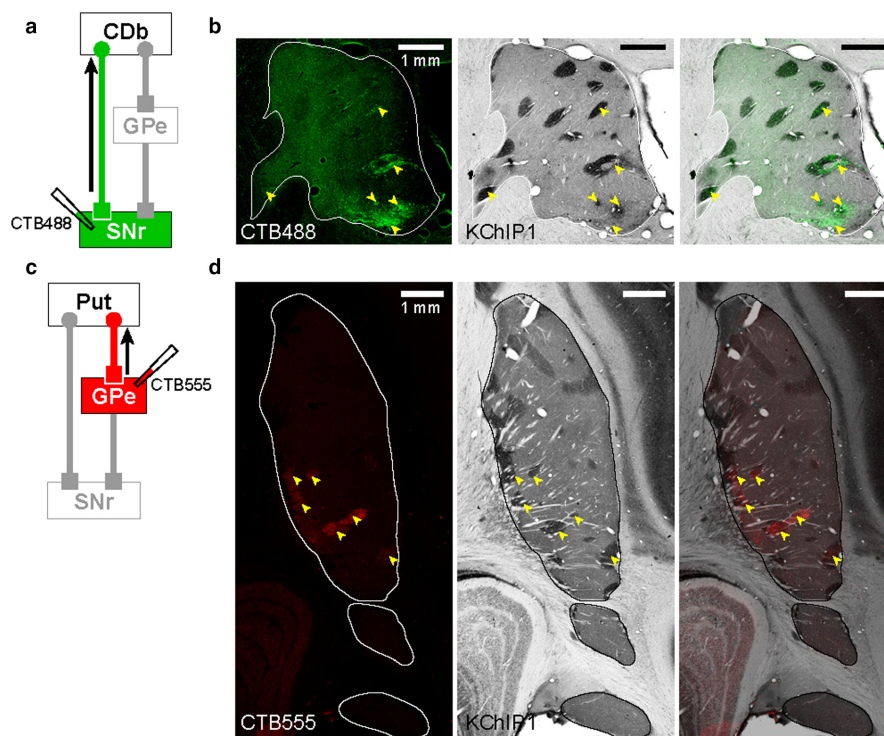

FIG. 6. cdlSNr- and cvGPe-projecting neurons in patches (striosomes). (a) Scheme of CTB488 injection site in cdlSNr of monkey AX. (b, left) CTB488-labeled cells in CDb (indicated by yellow arrowheads). (b, center) Patches (striosomes) in CDb were stained by KChIP1 immunostaining. (b, right) Overlaid image of two adjacent sections showed most labeled cells were localized in the patches of CDb. (c) Scheme of CTB555 injection site in cvGPe of monkey AX. (d, left) CTB555 labeled cells in Put (indicated by yellow arrowheads). (d, center) Patches (striosomes) in Put were stained by KChIP1 immunostaining. (d, right) Overlaid image of two adjacent sections showed most labeled cells were localized in the patches of Put.

A small but significant number of neurons in CDt and cvPut project to both cdlSNr and cvGPe

We found that neurons in the input structures in direct and indirect pathways were spatially intermingled. Then, do the same or different neurons project to cdlSNr and cvGPe? To address this question in monkey AX, we examined whether neurons in CDt and cvPut were double-labeled with FB and CTB555 which were injected in cdlSNr and cvGPe of the same hemisphere, respectively (Figure 9a), and found some double-labeled neurons (Figure 9b and c). We then
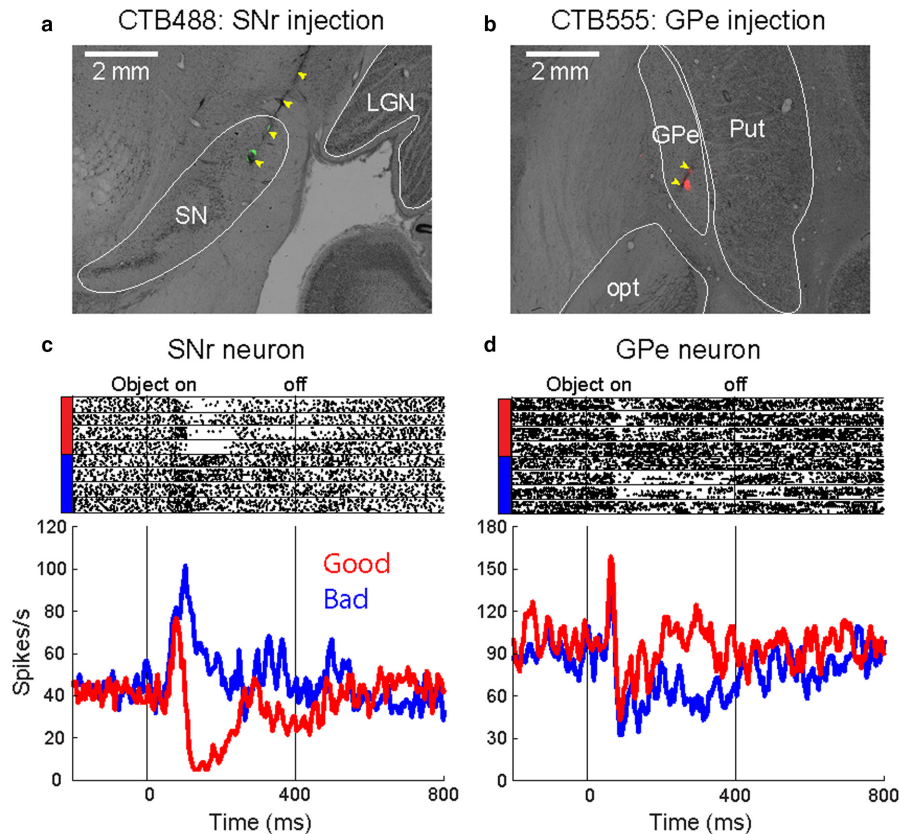
FIG. 7. Specific target-localized injection sites showing stable value coding in monkey CR. (a) Localized injection site in cdlSNr. CTB488 was locally injected in right cdlSNr (injectrode track indicated by yellow arrowheads). (b) Localized injection site in cvGPe. CTB555 was locally injected in right cvGPe (injectrode track indicated by yellow arrowheads). (c) An example neuronal activity encoding stable value. A neuron at the injection site in cdlSNr showed inhibition by good object presentation (red line) and excitation by bad object presentation (blue line). (d) An example neuronal activity encoding stable value. A neuron at the injection site in cvGPe showed excitation by good object presentation (red line) and inhibition by bad object presentation (blue line). Raster plot indicates spike response in individual trial. Peristimulus time histogram (PSTH) indicates the neuronal response aligned by object presentation onset.

examined CDt and cvPut in coronal brain slices along the rostral-caudal axis and identified all retrogradely labeled neurons (Figure 10). Double-labeled neurons were distributed in whole regions of CDt and cvPut (Figure 10a–c), though fewer in caudal regions (Figure 10d–e). In the other monkey (monkey CR), double-labeled neurons were also found in CDt and cvPut (Figure 8). Among neurons retrogradely labeled from cdlSNr, some were retrogradely labeled also from cvGPe: 7.4% ($n = 337/4548$; monkey AX) and 3.3% ($n = 27/825$; monkey CR). Among neurons retrogradely labeled from cvGPe, some were retrogradely labeled also from cdlSNr: 3.7% ($n = 337/9197$; monkey AX) and 13.6% ($n = 27/198$; monkey CR). Overall, double-labeled neurons among all retrogradely labeled neurons was 2.5% ($n = 337/13408$) in monkey AX and 2.7% (27/996) in monkey CR. These results showed that small but significant number of neurons in CDt and cvPut projected to both cdlSNr and cvGPe.

Discussion

Striatum tail: Common features between CDt and cvPut

Our data showed that CDt and cvPut share the same downstream circuits (Figure 11). Their targets are highly localized in two areas: cdlSNr and cvGPe. All of them are located in the caudal part of basal ganglia. The connections of the caudal basal ganglia are different from the rostral basal ganglia (Smith & Parent, 1986). Our

current and previous data (Kim et al., 2017), including electrophysiological data, suggested that cvGPe also has very localized target—cdlSNr (Figure 5b). These data are consistent with previous anatomical studies showing that GPe has direct projections to SNr in both rodents and primates (Kita, 2007; Kita & Kitai, 1994; Parent & Hazrati, 1995; Sato, Lavallee, Levesque, & Parent, 2000; ShammahLagnado, Alheid, & Heimer, 1996; Smith & Bolam, 1989, 1991). Furthermore, most neurons in cdlSNr project to SC which controls saccadic eye movements (Beckstead & Frankfurter, 1982; Francois, Percheron, Yelnik, & Heyner, 1985; Hikosaka & Wurtz, 1983; Yasuda & Hikosaka, 2015; Yasuda et al., 2012). Thus, these circuits, which are specialized for visuo-oculomotor behavior, are finally converged in cdlSNr–SC pathway. These data suggest that the combination of CDt and cvPut is a single functional area in the striatum, which may be called "striatum tail" (Figure 11). CDt and cvPut are regarded as different structures because they are separated by axonal tracts. The rostral parts of CD and Put are also separated by internal capsule. If axonal tracts are less distinct, CD and Put may not be distinctly separated, which is true in many animals other than primates (Marin, Smeets, & Gonzalez, 1998; Swanson, 2000).

The downstream circuits of the striatum tail process a very selective type of sensory information—visual objects. Medium spiny neurons in CDt respond to visual objects very selectively (Caan, Perrett, & Rolls, 1984; Yamamoto, Monosov, Yasuda, & Hikosaka, 2012; Yamamoto et al., 2013). Neurons in cvPut also show similar visual responses (Caan et al., 1984). These visual responses may be
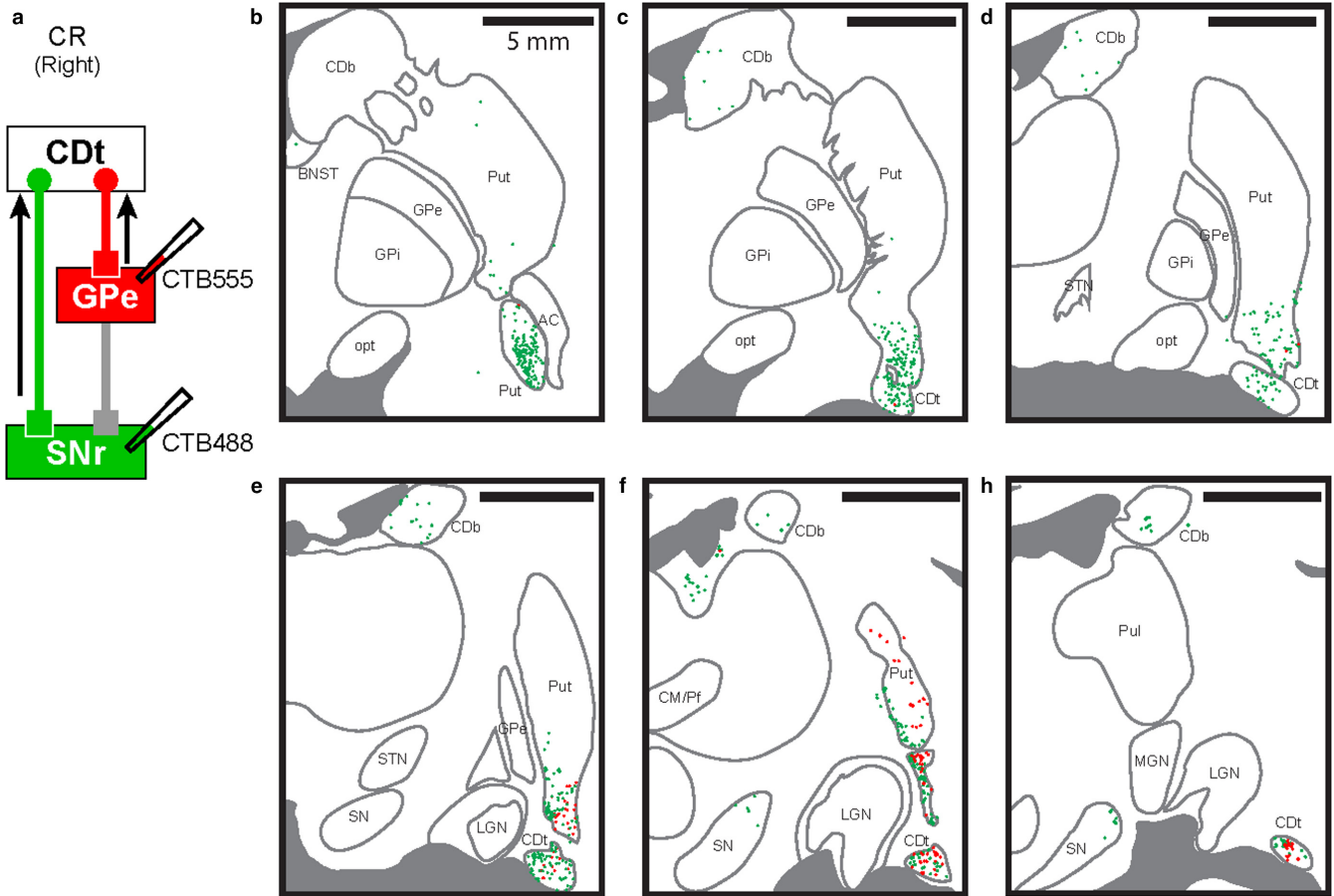
FIG. 8. cdlSNr- and cvGPe-projecting neurons were spatially intermingled in CDt and cvPut. (a) Scheme of injection sites in cdlSNr and cvGPe of monkey CR. CTB488 and CTB555 were injected in cdlSNr (green) and cvGPe (red), respectively. (b-g) Spatially intermingled projection neurons. Six coronal brain slices (P4, P6, P8, P10, P12 and P14) showed CTB488-positive (green dots) and CTB555-positive (red dots) neurons in the rostral-caudal axis. cdlSNr- and cvGPe-projecting neurons were spatially intermingled in cvPut and CDt (e-g). Series of six slices from rostral to caudal at 2 mm intervals.
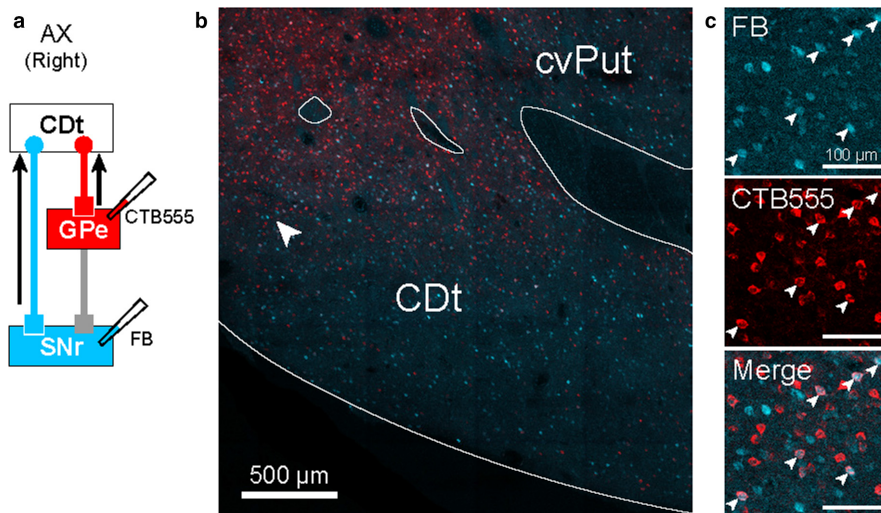

FIG. 9. An example section showing both cdlSNr- and cvGPe-projecting neurons in CDt. (a) Scheme of injection sites in cdlSNr and cvGPe of monkey AX. CTB555 and FB were injected in cvGPe and cdlSNr, respectively. (b) Distribution of cdlSNr- and cvGPe-projecting neurons in CDt. CTB555-positive signals (red) and FB-positive signals (cyan) were detected in the cvPut and CDt. (c) Both cdlSNr- and cvGPe-projecting neurons in CDt. Enlarged area where the neurons were retrogradely labeled with FB and CTB555, indicated by white arrowhead in (b). Double-labeled neurons are indicated by white arrowheads in the enlarged images.
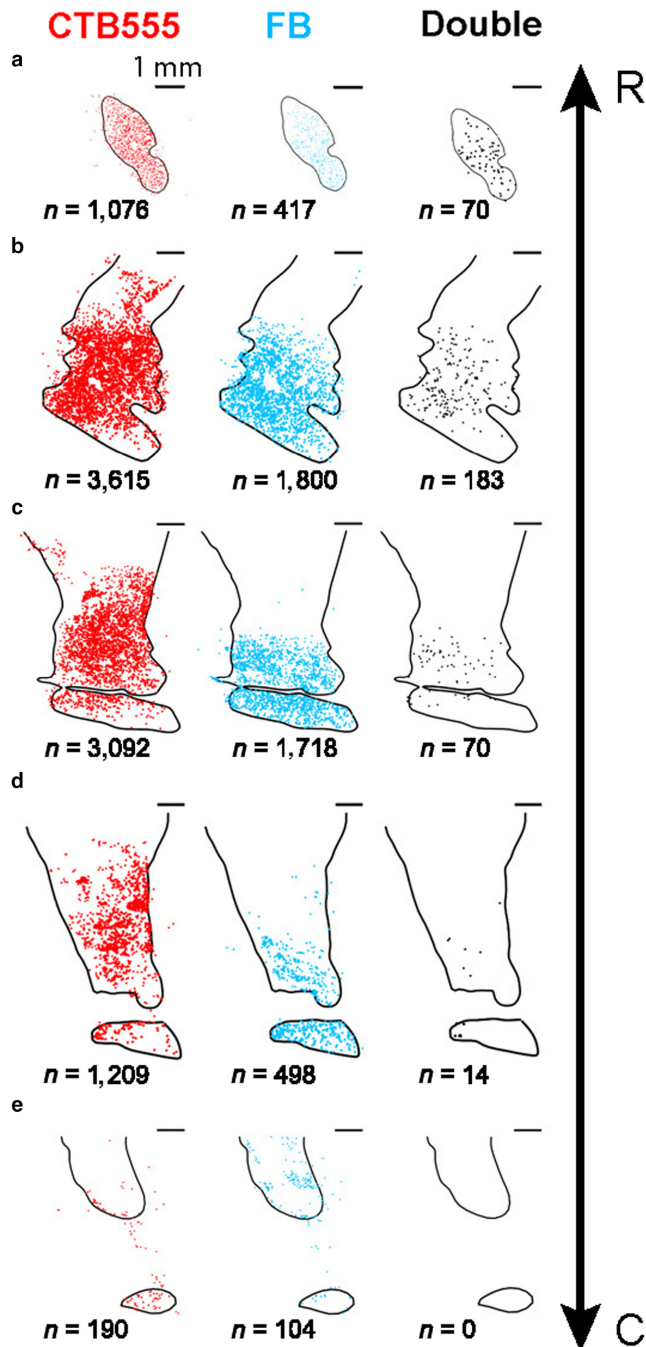
FIG. 10. Both cdlSNr- and cvGPe-projecting neurons in coronal slices. (a-e) Five coronal slices (P4, P6, P8, P10 and P12) in the rostral-caudal axis showed distribution of retrogradely labeled neurons with CTB555 (red), FB (cyan) and both (black). Numbers below the figures indicate the numbers of retrogradely labeled neurons in each slice. Note that the structure in (a) is the anterior part of cvPut (indicated by black arrowhead in Figure 4c). R: rostral, C: caudal.

FIG. 11. Schematic circuits of the caudal basal ganglia. "Striatum tail" (CDt and cvPut) receives inputs from visual cortex including the inferior temporal cortex. Neurons in the striatum tail project to cdlSNr and cvGPe in the direct and indirect pathways, respectively. Small but significant number of neurons in the striatum tail innervate both cdlSNr and cvGPe. These neurons may be direct or indirect pathway neurons with axon collaterals to cvGPe or cdlSNr, respectively. cvGPe projects to cdlSNr in two ways: directly or indirectly through cvSTN. cvSTN possibly receives inputs from pre-SMA. Amygdala areas and hypothalamus (VMH) may also be involved in these direct and indirect pathways. cdlSNr receives inputs through these direct and indirect pathways and send the information to SC for controlling saccadic eye movements.

neurons in CDt and cvPut to single neurons in cdlSNr and cvGPe. In fact, the tracers injected in localized sites in cdlSNr and cvGPe revealed retrogradely labeled neurons in an overall area CDt and cvPut, although their numbers are smaller (Figure 8).

In addition, neurons in the "striatum tail" circuit share other features due to the restricted connectivity: spatial selectivity and value coding. First, virtually all neurons in CDt, cvPut, cdlSNr and cvGPe respond to visual objects located somewhere on the contralateral side (Brown, Desimone, & Mishkin, 1995; Kim et al., 2017; Shin & Sommer, 2010; Yamamoto et al., 2012; Yasuda et al., 2012). Second, most of these neurons respond to visual objects differently depending on how they had been associated with different reward values historically (Kim et al., 2017; Yamamoto et al., 2013; Yasuda et al., 2012).

Double-labeled neurons in the striatum tail

We previously found that CDt, cdlSNr and cvGPe neurons have different patterns of value coding: cdlSNr neurons are inhibited by good objects (Yasuda et al., 2012), cvGPe neurons are inhibited by bad objects (Kim et al., 2017) and some CDt neurons are more excited by good objects, but others are more excited by bad objects (Kim & Hikosaka, 2013; Yamamoto et al., 2013). These results suggested that two groups of CDt neurons project selectively to cdlSNr and cvGPe: CDt neurons, which are excited by good objects, project to cdlSNr through the direct pathway; CDt neurons, which are excited by bad objects, project to cvGPe through the indirect pathway. Our current anatomical data support this hypothesis: cdlSNr-projecting neurons and cvGPe-projecting

explained by anatomical studies showing that the inferior temporal cortex projects to CDt and cvPut in primates (Griggs et al., 2017; Kemp & Powell, 1970; Saintcyr, Ungerleider, & Desimone, 1990; Yeterian & Vanhoesen, 1978). Due to the selective projections from CDt and cvPut, neurons in both cdlSNr and cvGPe respond to visual objects, but less selectively (Kim et al., 2017; Yasuda et al., 2012). This may be caused by the convergence of inputs from multiple
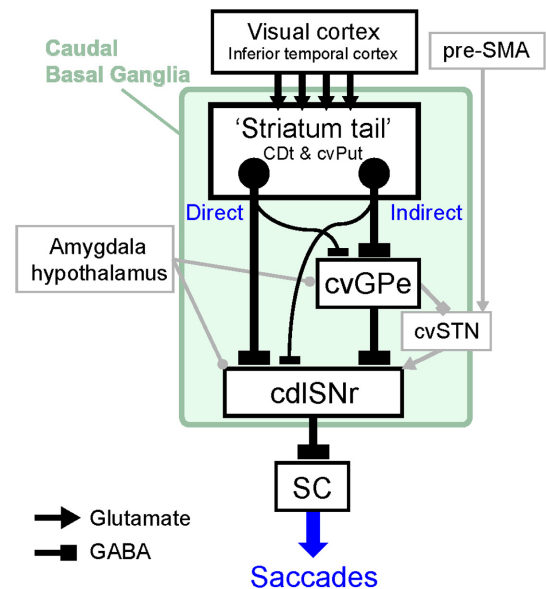
neurons are largely separate, although they are spatially intermingled (Figures 9 and 10). This result is consistent with previous anatomical studies based on retrograde tracing in primates (Flaherty & Graybiel, 1993).

However, we also found that a relatively small but significant proportion (<15%) of the "striatum tail" neurons project to both cdlSNr and cvGPe. Previous studies using single-cell labeling showed that most striatal neurons project to both GPe and SNr (Fujiyama et al., 2011; Kawaguchi, Wilson, & Emson, 1990; Levesque & Parent, 2005; Parent, Charara, & Pinault, 1995; Parent et al., 2000; Wu, Richard, & Parent, 2000). Thus, each CDt neuron may project to both cdlSNr and cvGPe, but with biased outputs to them (as illustrated in Figure 11). If the bias is strong, the neuron's soma may be single-labeled with a tracer originating from the dominant output site.

The biased (not exclusive) connections may be used for object representation based on the gradient of value. For example, CDt neurons projecting only to cdlSN may represent extremely good objects, while CDt neurons projecting to both cdlSNr and cvGPe, but more strongly to cdlSNr, may represent moderately good objects. The biased connections may be created through learning experience at the level of cdlSNr and cvGPe. Here is a hypothesis. Initially, CDt neurons project to both cdlSNr and cvGPe. One new object would activate a certain group of CDt neurons due to their object selectivity (Yamamoto et al., 2012). If the object is good, these CDt neurons would weaken their connections to cvGPe, and strengthen the connections to cdlSNr. The outcome of this mechanism (i.e., gradient levels of connections to cdlSNr vs. cvGPe) may be maintained stably as long-term memory, which is encoded by cdlSNr and cvGPe neurons (Kim et al., 2017; Yasuda et al., 2012). In fact, when there are several groups of objects with gradient values, monkeys discriminate them in a biased (not exclusive) manner: they make saccades more often to better objects and fixate gaze on them longer (Ghazizadeh, Griggs, & Hikosaka, 2016). This hypothetical mechanism will be further studied in near future.

Interaction between basal ganglia circuits through patches (striosomes)

In addition to the striatum tail, some neurons in other parts of the striatum (CDb, Put) projected to cdlSNr and cvGPe. Those retrogradely labeled cells were localized in patches (striosomes) (Figure 6), which is very different from the striatum tail where retrogradely labeled cells were mostly uniformly distributed. It has been shown that patches (striosomes) receive inputs mainly from the limbic cortex (Eblen & Graybiel, 1995) and the basal nucleus of the amygdala (Ragsdale & Graybiel, 1988), which suggest that emotional signals are transmitted to cdlSNr and cvGPe. This might be related to the data that most neurons in cdlSNr and cvGPe discriminate visual objects by their values stably and automatically and control saccadic eye movement (Kim et al., 2017; Yasuda et al., 2012). In this sense, the connection from patches (striosomes) may be involved in subconscious emotional behaviors (Tamietto & de Gelder, 2010).

This connection might also involve dopamine neurons. Since patches (striosomes) are known to project to dopamine neurons (Gerfen, 1984), the retrogradely labeled cells in the patches (striosomes) from cdlSNr might also reflect the connection to dopamine neurons. Notably, dopamine neurons close to cdlSNr encode reward values stably (not reward prediction error) and project to CDt (Kim, Ghazizadeh, & Hikosaka, 2015), where neurons encode object values stably and automatically (Kim & Hikosaka, 2013; Yamamoto

et al., 2013). Overall, the circuit originating from the striatum tail may be modulated by the inputs from other parts of the striatum through patches (striosomes).

Interaction of basal ganglia circuit with areas outside of the basal ganglia

So far, we have emphasized that the striatum tail circuit is a closed circuit anatomically and functionally. On the other hand, retrogradely labeled neurons were found in several brain areas, including STN, CeA, SLEA, BNST and VMH (Figures 3 and 4). These structures are outside the basal ganglia, except for STN. This might be caused by spreading of the injected tracer, especially into the putamen in case of cvGPe injection (Figure 2b). However, these structures were labeled more clearly after the restricted injection to cdlSNr (Figures 2a and 3c-h). Therefore, these areas are likely to project to cdlSNr and possibly to cvGPe.

These data suggest that a closed circuit in the basal ganglia controlling a specific behavior is open for brain areas outside of the basal ganglia (Figure 11). The striatum tail circuit chooses objects based on their values. However, such a decision needs to be modulated by internal body conditions and external environmental conditions. Then, the inputs from outside of the basal ganglia would be useful, such as the hypothalamus (VMH). The inputs from the amygdala areas (CeA, SLEA and BNST) may be useful to control the behavior based on motivation or stress (Davis, 1992; Murray, 2007; Paton, Belova, Morrison, & Salzman, 2006). Previous anatomical studies reported that the CeA neurons had axon collaterals to both the GPe and cdlSNr in cats (Shinonaga, Takada, & Mizuno, 1992), and these amygdala areas project to both cdlSNr and SNc in primates (Fudge & Haber, 2000, 2001; Price & Amaral, 1981). STN may modulate or switch behavior in uncertain conditions or in response to unexpected events (Isoda & Hikosaka, 2007, 2008; Monchi, Petrides, Strafella, Worsley, & Doyon, 2006). Indeed, the caudal-ventral part of STN (cvSTN), which included retrogradely labeled cells from cdlSNr (Figure 4c and d), plays a role in the switching functions (Isoda & Hikosaka, 2008). These results suggest that multiple circuits in the basal ganglia, each of which is involved in a specific behavior, interact with areas outside of the basal ganglia. Further studies are necessary to elucidate the involvements of these areas in the basal ganglia circuit.

Competing Interests

No conflicts of interest, financial or otherwise, are declared by the authors.

Data Accessibility

The data and materials presented in the current study can be available upon request by the corresponding author.

Author Contributions

H.A., H.F.K. and O.H. designed these experiments. H.A. preformed recording and injections. M.K.S. performed histology and staining. H.A. and A.G.

performed histology analysis and cell counting. H.A. prepared figures. H.A., H.F.K. and O.H. drafted manuscript.

Abbreviations

AC, anterior commissure; BNST, bed nucleus of the stria terminalis; C, caudal; CDb, caudate body; CD, caudate nucleus; cdlSNr, caudal-dorsal-lateral part of SNr; CDt, caudate tail; CeA, central nucleus of the amygdala; CM/Pf, centromedian-parafascicular nuclei; cvGPe, caudal-ventral part of GPe; cvPut, caudal-ventral part of Put; cvSTN, caudal-ventral part of STN; D, dorsal; GPe, globus pallidus externus; GPi, globus pallidus internus; LGN, lateral geniculate nucleus; LV, lateral ventricle; MGN, medial geniculate nucleus; Opt, optic tract; PAG, periaqueductal gray; Pul, pulvinar nuclei; Put, putamen; RN, red nucleus; R, rostral; SLEA, sublenticular extended amygdala; SNc, substantia nigra pars compacta; SNr, substantia nigra pars reticulata; SN, substantia nigra; STN, subthalamic nucleus; St, stria terminalis; VMH, ventromedial hypothalamus; V, ventral.

References

Beckstead, R. M., & Frankfurter, A. (1982). The distribution and some morphological features of substantia nigra neurons that project to the thalamus, superior colliculus and pedunculopontine nucleus in the monkey. *Neuroscience*, 7, 2377–2388.

Brown, V. J., Desimone, R., & Mishkin, M. (1995). Responses of cells in the tail of the caudate nucleus during visual discrimination learning. *Journal of Neurophysiology*, 74, 1083–1094.

Caan, W., Perrett, D. I., & Rolls, E. T. (1984). Responses of striatal neurons in the behaving monkey. 2. Visual processing in the caudal neostriatum. *Brain Research*, 290, 53–65.

Chen, S., & AstonJones, G. (1998). Axonal collateral-collateral transport of tract tracers in brain neurons: False anterograde labelling and useful tool. *Neuroscience*, 82, 1151–1163.

Cui, G., Jun, S. B., Jin, X., Pham, M. D., Vogel, S. S., Lovinger, D. M., & Costa, R. M. (2013). Concurrent activation of striatal direct and indirect pathways during action initiation. *Nature*, 494, 238–242.

Davis, M. (1992). The role of the amygdala in fear and anxiety. *Annual Review of Neuroscience*, 15, 353–375.

DeLong, M. R. (1990). Primate models of movement disorders of basal ganglia origin. *Trends in Neurosciences*, 13, 281–285.

Eblen, F., & Graybiel, A. M. (1995). Highly restricted origin of prefrontal cortical inputs to striosomes in the macaque monkey. *Journal of Neuroscience*, 15, 5999–6013.

Ferguson, S. M., Eskenazi, D., Ishikawa, M., Wanat, M. J., Phillips, P. E., Dong, Y., . . . Neumaier, J. F. (2011). Transient neuronal inhibition reveals opposing roles of indirect and direct pathways in sensitization. *Nature Neuroscience*, 14, 22–24.

Flaherty, A. W., & Graybiel, A. M. (1993). Output architecture of the primate putamen. *Journal of Neuroscience*, 13, 3222–3237.

Francois, C., Percheron, G., Yelnik, J., & Heyner, S. (1985). A histological atlas of the macaque (Macaca mulatta) substantia nigra in ventricular coordinates. *Brain Research Bulletin*, 14, 349–367.

Fudge, J. L., & Haber, S. N. (2000). The central nucleus of the amygdala projection to dopamine subpopulations in primates. *Neuroscience*, 97, 479–494.

Fudge, J. L., & Haber, S. N. (2001). Bed nucleus of the stria terminalis and extended amygdala inputs to dopamine subpopulations in primates. *Neuroscience*, 104, 807–827.

Fujiyama, F., Sohn, J., Nakano, T., Furuta, T., Nakamura, K. C., Matsuda, W., & Kaneko, T. (2011). Exclusive and common targets of neostriatofugal projections of rat striosome neurons: A single neuron-tracing study using a viral vector. *The European Journal of Neuroscience*, 33, 668–677.

Gerfen, C. R. (1984). The neostriatal mosaic – compartmentalization of corticostriatal input and striatonigral output systems. *Nature*, 311, 461–464.

Ghazizadeh, A., Griggs, W., & Hikosaka, O. (2016). Ecological origins of object salience: Reward, uncertainty, aversiveness, and novelty. *Front Neurosci-Switz*, 10, 378.

Graybiel, A. M., & Ragsdale, C. W. (1978). Histochemically distinct compartments in striatum of human, monkey, and cat demonstrated by acetylthiocholinesterase staining. *Proceedings of the National Academy of Sciences of the United States of America*, 75, 5723–5726.

Griggs, W. S., Kim, H. F., Ghazizadeh, A., Costello, M. G., Wall, K. M., & Hikosaka, O. (2017). Flexible and stable value coding areas in caudate

head and tail receive anatomically distinct cortical and subcortical inputs. *Frontiers in Neuroanatomy*, 11, 106.

Hikida, T., Kimura, K., Wada, N., Funabiki, K., & Nakanishi, S. (2010). Distinct roles of synaptic transmission in direct and indirect striatal pathways to reward and aversive behavior. *Neuron*, 66, 896–907.

Hikosaka, O., Ghazizadeh, A., Griggs, W., & Amita, H. (2017). Parallel basal ganglia circuits for decision making. *Journal of Neural Transmission*, 125, 515–529.

Hikosaka, O., Takikawa, Y., & Kawagoe, R. (2000). Role of the basal ganglia in the control of purposive saccadic eye movements. *Physiological Reviews*, 80, 953–978.

Hikosaka, O., & Wurtz, R. H. (1983). Visual and oculomotor functions of monkey substantia nigra pars reticulata. 4. relation of substantia nigra to superior colliculus. *Journal of Neurophysiology*, 49, 1285–1301.

Isoda, M., & Hikosaka, O. (2007). Switching from automatic to controlled action by monkey medial frontal cortex. *Nature Neuroscience*, 10, 240–248.

Isoda, M., & Hikosaka, O. (2008). Role for subthalamic nucleus neurons in switching from automatic to controlled eye movement. *The Journal of Neuroscience: The Official Journal of the Society for Neuroscience*, 28, 7209–7218.

Isomura, Y., Takekawa, T., Harukuni, R., Handa, T., Aizawa, H., Takada, M., & Fukai, T. (2013). Reward-modulated motor information in identified striatum neurons. *Journal of Neuroscience*, 33, 10209–10220.

Jin, X., Tecuapetla, F., & Costa, R. M. (2014). Basal ganglia subcircuits distinctively encode the parsing and concatenation of action sequences. *Nature Neuroscience*, 17, 423–430.

Kawaguchi, Y., Wilson, C. J., & Emson, P. C. (1990). Projection subtypes of rat neostriatal matrix cells revealed by intracellular injection of biocytin. *Journal of Neuroscience*, 10, 3421–3438.

Kemp, J. M., & Powell, T. P. S. (1970). Cortico-striate projection in monkey. *Brain*, 93, 525–546.

Kim, H. F., Amita, H., & Hikosaka, O. (2017). Indirect pathway of caudal basal ganglia for rejection of valueless visual objects. *Neuron*, 94(920–930), e923.

Kim, H. F., Ghazizadeh, A., & Hikosaka, O. (2014). Separate groups of dopamine neurons innervate caudate head and tail encoding flexible and stable value memories. *Frontiers in Neuroanatomy*, 8, 120.

Kim, H. F., Ghazizadeh, A., & Hikosaka, O. (2015). Dopamine neurons encoding long-term memory of object value for habitual behavior. *Cell*, 163, 1165–1175.

Kim, H. F., & Hikosaka, O. (2013). Distinct basal ganglia circuits controlling behaviors guided by flexible and stable values. *Neuron*, 79, 1001–1010.

Kincaid, A. E., Penney, J. B., Young, A. B., & Newman, S. W. (1991). The globus-pallidus receives a projection from the parafascicular nucleus in the rat. *Brain Research*, 553, 18–26.

Kita, H. (2007). Globus pallidus external segment. *Gaba and the Basal Ganglia: From Molecules to Systems*, 160, 111–133.

Kita, H., & Kitai, S. T. (1994). The morphology of globus-pallidus projection neurons in the rat – an intracellular staining study. *Brain Research*, 636, 308–319.

Kravitz, A. V., Freeze, B. S., Parker, P. R. L., Kay, K., Thwin, M. T., Deisseroth, K., & Kreitzer, A. C. (2010). Regulation of parkinsonian motor behaviours by optogenetic control of basal ganglia circuitry. *Nature*, 466, 622–626.

Kravitz, A. V., Tye, L. D., & Kreitzer, A. C. (2012). Distinct roles for direct and indirect pathway striatal neurons in reinforcement. *Nature Neuroscience*, 15, 816–818.

Levesque, M., & Parent, A. (2005). The striatofugal fiber system in primates: A reevaluation of its organization based on single-axon tracing studies. *Proceedings of the National Academy of Sciences of the United States of America*, 102, 11888–11893.

Marin, O., Smeets, W. J. A. J., & Gonzalez, A. (1998). Evolution of the basal ganglia in tetrapods: A new perspective based on recent studies in amphibians. *Trends in Neurosciences*, 21, 487–494.

Mikula, S., Parrish, S. K., Trimmer, J. S., & Jones, E. G. (2009). Complete 3D visualization of primate striosomes by KChIP1 immunostaining. *Journal of Comparative Neurology*, 514, 507–517.

Mink, J. W. (1996). The basal ganglia: Focused selection and inhibition of competing motor programs. *Progress in Neurobiology*, 50, 381–425.

Monchi, O., Petrides, M., Strafella, A. P., Worsley, K. J., & Doyon, J. (2006). Functional role of the basal ganglia in the planning and execution of actions. *Annals of Neurology*, 59, 257–264.

Murray, E. A. (2007). The amygdala, reward and emotion. *Trends in Cognitive Sciences*, 11, 489–497.

Parent, A., Charara, A., & Pinault, D. (1995). Single striatofugal axons arborizing in both pallidal segments and in the substantia nigra in primates. *Brain Research*, **698**, 280–284.

Parent, A., & Hazrati, L. N. (1995). Functional-anatomy of the basal ganglia. 2. The place of subthalamic nucleus and external pallidum in basal ganglia circuitry. *Brain Research Reviews*, **20**, 128–154.

Parent, M., & Parent, A. (2005). Single-axon tracing and three-dimensional reconstruction of centre median-parafascicular thalamic neurons in primates. *Journal of Comparative Neurology*, **481**, 127–144.

Parent, A., Sato, F., Wu, Y., Gauthier, J., Levesque, M., & Parent, M. (2000). Organization of the basal ganglia: The importance of axonal collateralization. *Trends in Neurosciences*, **23**, S20–S27.

Paton, J. J., Belova, M. A., Morrison, S. E., & Salzman, C. D. (2006). The primate amygdala represents the positive and negative value of visual stimuli during learning. *Nature*, **439**, 865–870.

Price, J. L., & Amaral, D. G. (1981). An autoradiographic study of the projections of the central nucleus of the monkey amygdala. *Journal of Neuroscience*, **1**, 1242–1259.

Ragsdale, C. W., & Graybiel, A. M. (1988). Fibers from the basolateral nucleus of the amygdala selectively innervate striosomes in the caudate-nucleus of the cat. *Journal of Comparative Neurology*, **269**, 506–522.

Royce, G. J., & Mourey, R. J. (1985). Efferent connections of the centromedian and parafascicular thalamic nuclei – an autoradiographic investigation in the cat. *Journal of Comparative Neurology*, **235**, 277–300.

Sadikot, A. F., Parent, A., Smith, Y., & Bolam, J. P. (1992). Efferent connections of the centromedian and parafascicular thalamic nuclei in the squirrel-monkey – a light and electron-microscopic study of the thalamostriatal projection in relation to striatal heterogeneity. *Journal of Comparative Neurology*, **320**, 228–242.

Saintcyr, J. A., Ungerleider, L. G., & Desimone, R. (1990). Organization of visual cortical inputs to the striatum and subsequent outputs to the pallidonigral complex in the monkey. *Journal of Comparative Neurology*, **298**, 129–156.

Sato, F., Lavallee, P., Levesque, M., & Parent, A. (2000). Single-axon tracing study of neurons of the external segment of the globus pallidus in primate. *Journal of Comparative Neurology*, **417**, 17–31.

ShammahLagnado, S. J., Alheid, G. F., & Heimer, L. (1996). Efferent connections of the caudal part of the globus pallidus in the rat. *Journal of Comparative Neurology*, **376**, 489–507.

Shin, S. Y., & Sommer, M. A. (2010). Activity of neurons in monkey globus pallidus during oculomotor behavior compared with that in substantia nigra pars reticulata. *Journal of Neurophysiology*, **103**, 1874–1887.

Shinonaga, Y., Takada, M., & Mizuno, N. (1992). Direct projections from the central amygdaloid nucleus to the globus-pallidus and substantia-nigra in the cat. *Neuroscience*, **51**, 691–703.

Smith, Y., & Bolam, J. P. (1989). Neurons of the substantia nigra reticulata receive a dense gaba-containing input from the globus pallidus in the rat. *Brain Research*, **493**, 160–167.

Smith, Y., & Bolam, J. P. (1991). Convergence of synaptic inputs from the striatum and the globus-pallidus onto identified nigrocollicular cells in the rat – a double anterograde labeling study. *Neuroscience*, **44**, 45–73.

Smith, Y., & Parent, A. (1986). Differential connections of caudate-nucleus and putamen in the squirrel-monkey (Saimiri-Sciureus). *Neuroscience*, **18**, 347–371.

Swanson, L. W. (2000). Cerebral hemisphere regulation of motivated behavior. *Brain Research*, **886**, 113–164.

Tamietto, M., & de Gelder, B. (2010). Neural bases of the non-conscious perception of emotional signals. *Nature Reviews Neuroscience*, **11**, 697–709.

Wu, Y., Richard, S., & Parent, A. (2000). The organization of the striatal output system: A single-cell juxtacellular labeling study in the rat. *Neuroscience Research*, **38**, 49–62.

Yamamoto, S., Kim, H. F., & Hikosaka, O. (2013). Reward value-contingent changes of visual responses in the primate caudate tail associated with a visuomotor skill. *Journal of Neuroscience*, **33**, 11227–11238.

Yamamoto, S., Monosov, I. E., Yasuda, M., & Hikosaka, O. (2012). What and where information in the caudate tail guides saccades to visual objects. *Journal of Neuroscience*, **32**, 11005–11016.

Yasuda, M., & Hikosaka, O. (2015). Functional territories in primate substantia nigra pars reticulata separately signaling stable and flexible values. *Journal of Neurophysiology*, **113**, 1681–1696.

Yasuda, M., Yamamoto, S., & Hikosaka, O. (2012). Robust representation of stable object values in the oculomotor basal ganglia. *Journal of Neuroscience*, **32**, 16917–16932.

Yeterian, E. H., & Vanhoesen, G. W. (1978). Cortico-striate projections in rhesus-monkey – organization of certain cortico-caudate connections. *Brain Research*, **139**, 43–63.